

A study of the two northern open clusters NGC 1582 and NGC 1663 ^{*}, ^{**}

Gustavo Baume^{1,2}, Sandro Villanova¹ and Giovanni Carraro¹

¹ Dipartimento di Astronomia, Università di Padova, Vicolo Osservatorio 2, I-35122 Padova, Italy

² Facultad de Ciencias Astronómicas y Geofísicas de la UNLP, IALP-CONICET, Paseo del Bosque s/n, La Plata, Argentina

Received ^{**}; accepted ^{**}

Abstract. We present CCD $UBV(I)_C$ observations obtained in the field of the previously unstudied northern open clusters NGC 1582 and NGC 1663. For the former, we also provide high-resolution spectra of the brightest stars and complement our data with Two-Micron All-Sky-Survey (2MASS) near-infrared photometry and with astrometric data from the Tycho-2 catalog.

From the analysis of all these data, we argue that NGC 1582 is a very poor, quite large and heavily contaminated open cluster. It turns out to have a reddening $E_{B-V} = 0.35 \pm 0.03$, to be situated 1100 ± 100 pc from the Sun and to have an age of 300 ± 100 Myr.

On the other hand, we were not able to unambiguously clarify the nature of NGC 1663. By assuming it is a real cluster and from the analysis of its photometric diagrams, we found a color excess value $E_{B-V} = 0.20$, an intermediate age value (~ 2000 Myr) and a distance of about 700 pc. The distribution of the stars in the region however suggests we are probably facing an open cluster remnant. As an additional result, we obtained aperture photometry of three previously unclassified galaxies placed in the field of NGC 1663 and performed a preliminary morphological classification of them.

Key words. Galaxy: open clusters and associations: individual: NGC 1582 and NGC 1663 – open clusters and associations: general

1. Introduction

This study is part of a long term project aimed at providing accurate CCD photometry for poorly known or unstudied northern open clusters (Carraro 2002a, and references therein). Here we focus our attention on the open clusters NGC 1582 and NGC 1663. Both objects have never been studied before, apart from the identification and a preliminary estimate of their angular size. Their basic data are summarized in Table 1.

By inspecting the finding charts of these two clusters (see Figs. 2 and 10), we notice mainly that:

- NGC 1582 lies in a region where several bright stars are present, many of them with a Henry Draper (HD) classification. The cluster appears as a weak concentration of a small group of bright stars well mixed with the

very rich Galactic disk field star population toward its direction. This renders it difficult to study objects like this, and this is -we guess- the main reason for which this object has been almost neglected up to now;

- NGC 1663, which is located fairly high above the galactic plane, suffers from less contamination, and resembles the kind of objects recently suggested by Bica et al. (2001) to be Probable Open Cluster Remnants (POCRs).

In this study we would like to address the issue of the real nature of these two objects and to provide the first estimate of their fundamental parameters, namely distance, reddening, size and age. Therefore, we performed multicolor $UBV(I)_C$ photometry for both, and high-resolution spectroscopy for some stars in the NGC 1582 field. We also complement and cross-correlate our data with the 2MASS catalog and with proper motions from the Tycho-2 catalog (Høg et al. 2000), whenever available.

The plan of this study is as follows: In Sect. 2 we briefly present the observations and data reduction. In Sect. 3 and Sect. 4 we illustrate our analysis and results for NGC

Send offprint requests to: baume@pd.astro.it

^{*} Based on observations carried out at Mt Ekar, Asiago, Italy

^{**} Data is only available in electronic form at the CDS via anonymous ftp to cdsarc.u-strasbg.fr (130.79.128.5) or via <http://cdsweb.u-strasbg.fr/cgi-bin/qcat?J/A+A/>

Table 1. Basic data of the observed objects.

<i>Name</i>	α_{2000}	δ_{2000}	l	b
NGC 1582	04:32:15.4	+43:50:43	159.30°	-2.89°
NGC 1663	04:49:24.3	+13:08:27	185.92°	-19.65°

Table 2. Journal of observations of NGC 1582, NGC 1663 and standard star fields together with calibration coefficients (November 8, 2002).

Field	Filter	Exposure time			Seeing	Airmass
		[sec.]			[η]	
NGC 1582	U	900x2	180	20	2.5	1.196
	B	600	60	10	2.3	1.230
	V	300	30	5	2.4	1.255
	I	300	30	5	2.1	1.274
NGC 1663	U	900x2	-	-	2.5	1.348
	B	600	60	-	2.4	1.215
	V	300	30	3	2.2	1.188
	I	300	30	3	2.0	1.190
PG 0231+051	U	800			2.5	1.348
	B	300			2.4	1.324
	V	60			2.2	1.316
	I	90			2.2	1.315
PG 2213-006	U	600			2.5	1.447
	B	150			2.3	1.457
	V	30			2.3	1.465
	I	30			2.3	1.472
Calibration coefficients	u_1	$+3.861 \pm 0.015$			b_1	$+1.602 \pm 0.004$
	u_2	-0.142 ± 0.022			b_2	$+0.038 \pm 0.006$
	u_3	$+0.58$			b_3	$+0.29$
	v_{1bv}	$+1.003 \pm 0.014$			i_1	$+1.691 \pm 0.044$
	v_{2bv}	-0.016 ± 0.018			i_2	$+0.057 \pm 0.043$
	v_3	$+0.16$			i_3	$+0.08$
	v_{1vi}	$+1.002 \pm 0.016$				
	v_{2vi}	-0.013 ± 0.016				

1582 and NGC 1663, respectively. Sect. 5 is dedicated to a preliminary analysis of three previously unclassified galaxies in the field of NGC 1663. Finally, in Sect. 6 we draw our conclusions.

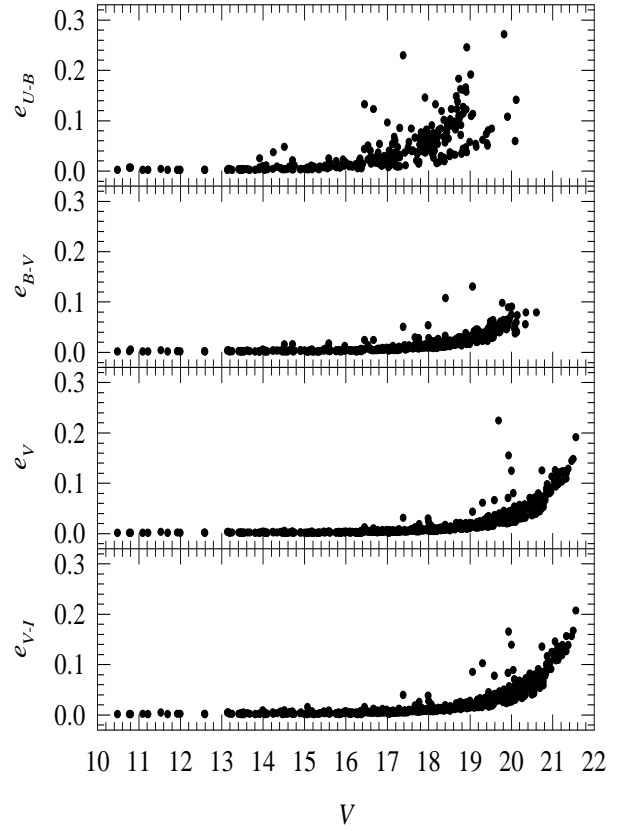
2. Observations and data reduction

2.1. Photometry

CCD $UBV(I)_C$ observations were carried out with the AFOSC camera at the 1.82 m Copernico telescope of Cima Ekar (Asiago, Italy), in the photometric night of November 8, 2002. AFOSC samples a $8'.14 \times 8'.14$ field in a $1K \times 1K$ nitrogen-cooled thinned CCD.

Details of the observations are listed in Table 2, where the observed fields are reported together with the exposure times, the typical seeing values and the air masses. Figs. 2 and 10 show the finding charts of the NGC 1582 and NGC 1663 regions respectively, indicating the covered areas and the object angular sizes. The data has been reduced with the IRAF[†] packages CCDRED, DAOPHOT, and PHOTCAL using the point spread function (PSF)

[†] IRAF is distributed by NOAO, which are operated by AURA under cooperative agreement with the NSF.

**Fig. 1.** Photometric errors in V magnitude and $U - B$, $B - V$ and $V - I$ colours as a function of V .

method (Stetson 1987). The calibration equations obtained by observing Landolt (1992) PG 0231+051 and PG 2213-006 fields during the night, are:

$$u = U + u_1 + u_2(U - B) + u_3X \quad (1)$$

$$b = B + b_1 + b_2(B - V) + b_3X \quad (2)$$

$$v = V + v_{1bv} + v_{2bv}(B - V) + v_3X \quad (3)$$

$$v = V + v_{1vi} + v_{2vi}(V - I) + v_3X \quad (4)$$

$$i = I + i_1 + i_2(V - I) + i_3X \quad (5)$$

where $UBVI$ are standard magnitudes, $ubvi$ are the instrumental ones, X is the airmass and the used coefficients are presented at the bottom of Table 2. As for V magnitudes, when B magnitude was available, we used expression (3) to compute them, elsewhere expression (4) was used. The standard stars in these fields provide a very good color coverage, essential to obtain reliable transformations. For the extinction coefficients, we assumed the typical values for the Asiago Observatory (u_3 , b_3 , v_3 and i_3 values in Table 2, Desidera et al. 2002[†]). Photometric global errors have been estimated following Patat & Carraro (2001) and their trends against V magnitude are shown in Fig. 1.

[†] <http://www.pd.astro.it/Asiago/2000/2300/2310.html>

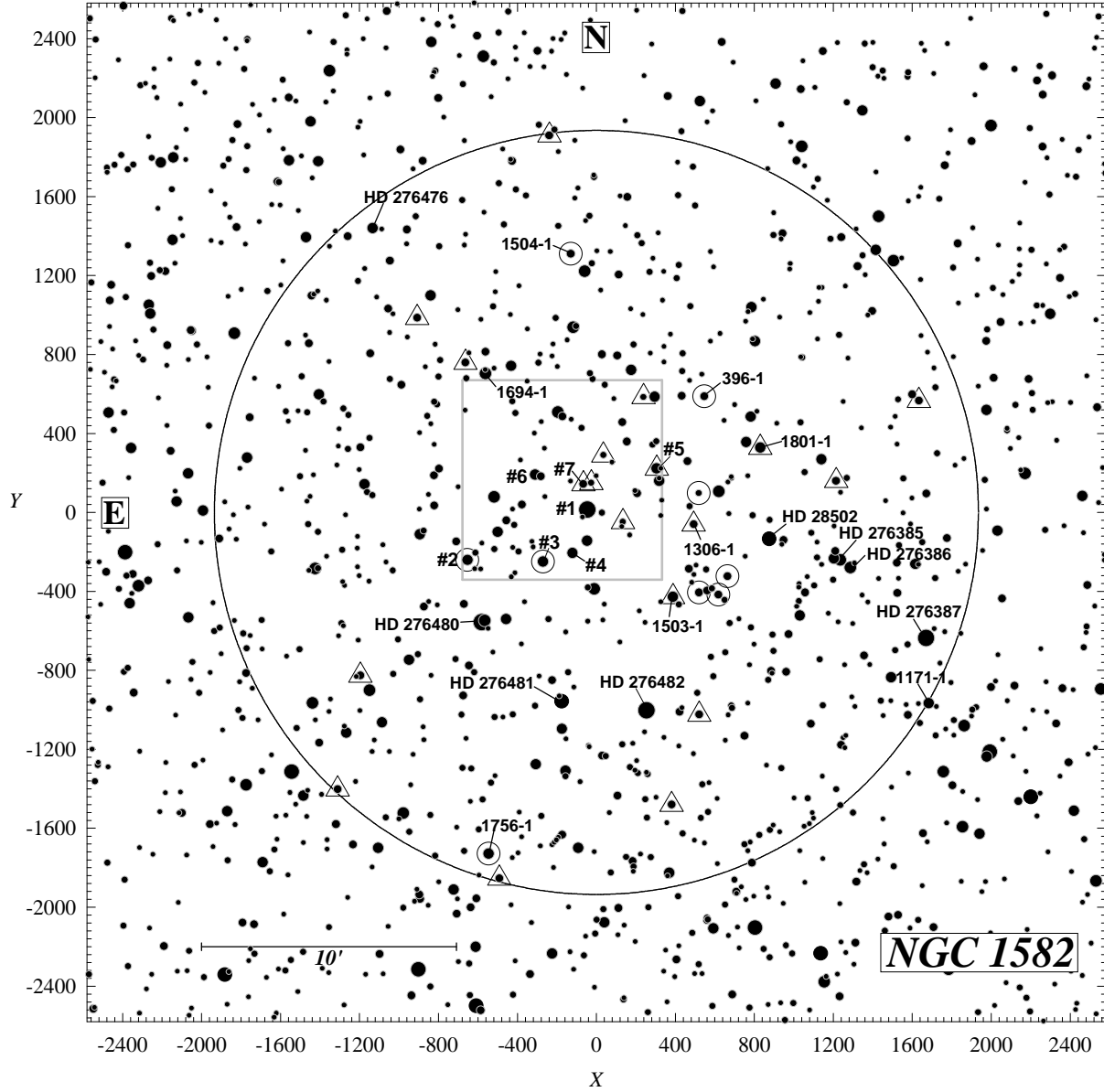


Fig. 2. Finding chart of the NGC 1582 region ($40' \times 40'$ and J filter). The black solid circle, $15'$ in radius, indicates the adopted angular size for the cluster (see Sect. 3.1 and Fig. 3). The grey square indicates the area covered from Asiago. Adopted cluster members and probable cluster members are shown with small circles and triangles, respectively. For a coordinate reference, the center ($X = 0$; $Y = 0$) corresponds to the cluster coordinates (see Table 1) and each X - Y unit is $0''.465$.

2.2. Spectroscopy

High-resolution ($R \approx 30,000$) spectra of 10 stars (see Table 3 and Fig. 5) in the field of NGC 1582 were obtained during the nights of January 14-15 and February 14, 2003, using the REOSC Echelle Spectrograph attached to the 1.82 m telescope of Asiago Astronomical Observatory. This instrument works with a Thomson 1024×1024 CCD and the allowed wavelength coverage is approximately $4500 - 6650 \text{ \AA}$. Details on this instrument are given in Munari & Zwitter (1994) and on the Asiago Observatory Home page[†].

The exposure times were 45 minutes for all the stars. In order to improve the signal-to-noise ratio, two exposures were taken for each star reaching at the end S/N values up to 70. The data have been reduced with the IRAF package ECHELLE using thorium lamp spectra for wavelength calibration purposes. By comparing final known sky line positions along the spectra we derived an error of about 0.01 \AA .

Spectra were classified mainly on the basis of the intensity of the Fe, H and He lines -depending on the spectral type- and by comparing them with spectrophotometric standards. The results are shown in Fig. 5, where we plot

[†] <http://www.pd.astro.it/Asiago/2000/2300/2320.html>

Table 3. Some bright stars in the region of NGC 1582.

#	2MASS ID. Tycho-2 ID. HD/GSC ID.	X Y	α_{2000} δ_{2000}	V	$B - V$ $U - B$ $V - I$	E_{B-V} E_{U-B} E_{V-I}	J	$J - K$	$\mu_{\alpha} \cos(\delta)$ μ_{δ} V_R	SC	Memb.
–	–	1671.0	04:31:3.24	8.61 _T	1.59 _T	0.26	–	–	1.7±1.2	K7 V	<i>nm</i>
	TYC 2892-803-1	-636.3	43:45:55.0		1.40 _C	0.19			-6.1±1.2		
	HD 276387				1.94 _C	0.33			41.4±1.0		
–	J0431376+434944	876.0	04:31:37.6	8.69 _T	0.23 _T	0.33	8.06	0.15	1.6±1.0	B8 V p	<i>nm</i>
	TYC 2892-510-1	-134.4	43:49:44.6		-0.06 _C	0.24			-2.5±1.1		
	HD 28502				0.30 _C	0.56			-21.0±3.0		
–	J0432225+434316	-175.9	04:32:22.5	9.33 _T	0.20 _T	0.33	8.71	-0.02	3.5±1.0	B6 V	<i>nm</i>
	TYC 2892-1450-1	-957.8	43:43:16.7		-0.18 _C	0.25			-4.3±1.0		
	HD 276481				0.32 _H	0.46			-16.0±3.0		
1	J0432173+435049	-45.9	04:32:17.3	10.77	2.01	–	6.75	1.22	–	M3-7 V	<i>nm</i>
	TYC 2892-1209-1	14.1	43:50:49.2		2.52	–			–		
	GSC 02892-01209				2.47	–			-26.4±1.6		
2	J0432433+434847	-654.1	04:32:43.3	10.80	0.33	0.35	10.02	0.17	0.6±1.4	A0 V *	<i>m</i>
	TYC 2892-354-1	-241.6	43:48:47.7		0.32	0.34			-5.3±1.4		
	HD 276479				0.46	0.47			7.5±2.2		
–	0432381+433716	-545.4	04:32:38.1	10.81 _T	0.22 _T	0.34	10.23	0.06	-2.7±1.4	B7 V	<i>m</i>
	TYC 2892-1756-1	-1729.7	43:37:16.0		-0.12 _C	0.25			-3.0±1.3		
	GSC 02892-01756				0.30 _C	0.42			4.9±1.0		
3	J0432269+434845	-270.2	04:32:26.9	11.09	0.31	0.38	10.39	0.19	0.8±1.5	B9 V p	<i>m</i>
	TYC 2892-1365-1	-249.8	43:48:45.5		0.10	0.30			-6.0±1.5		
	GSC 02892-01365				0.39	0.45			4.2±2.1		
4	J0432205+434906	-121.1	04:32:20.5	11.22	0.29	0.40	10.59	0.11	2.7±1.5	B8 V	<i>nm</i>
	TYC 2892-1195-1	-206.0	43:49:06.5		0.06	0.40			0.8±1.4		
	GSC 02892-01195				0.35	0.45			-37.0±3.0		
–	0431398+435319	830.6	04:31:39.8	11.35 _T	0.37 _T	0.47	10.76	0.21	-3.0±1.6	B8 V *	<i>pm</i>
	TYC 2892-1801-1	328.0	43:53:19.4		0.05 _C	0.35			-0.1±1.6		
	GSC 02892-01801				0.49 _C	0.59			-25.0±10.0		
–	0431025+434321	1684.0	04:31:02.5	11.43 _T	0.37 _T	0.32	10.89	0.13	-2.2±1.8	A2 V	<i>nm</i>
	TYC 2892-1171-1	-967.2	43:43:21.2		0.28 _C	0.23			-1.8±1.8		
	–				0.45 _C	0.39			-21.0±5.0		
5	J0432023+435228	306.1	04:32:02.3	11.53	0.41	0.35	10.71	0.22	-1.7±2.0	–	<i>pm</i>
	TYC 2892-225-1	223.0	43:52:28.1		0.36	0.26			-15.2±1.9		
	–				0.49	–			–		
6	J0432288+435210	-309.4	04:32:28.8	11.93	0.71	–	10.62	0.44	–	–	<i>nm</i>
	–	190.4	43:52:10.2		0.31	–			–		
	–				0.80	–			–		
7	J0432183+435149	-66.2	04:32:18.3	12.00	0.45	0.35	11.11	0.22	-5.8±1.9	–	<i>pm</i>
	TYC 2892-1159-1	143.8	43:51:49.6		0.35	0.26			1.0±1.8		
	–				0.51	–			–		

Notes:

- Letters *T*, *H* and *C* indicate data obtained from Tycho-2, Hipparcos catalog or computed according to the spectral classification (see text) respectively.
- Proper motion and radial velocity values are expressed in mas/yr and km/s respectively.
- Spectral classification (*SC*) was obtained from Asiago observations. Asterisks indicate probable binary stars.
- Membership (Memb.) is assigned as described in Sect. 3.4.

3.2. Proper motions and radial velocities

Important information on the kinematics of the brightest stars in and around NGC 1582 field can be derived from the study of proper motions and radial velocities. The former are available in the Tycho-2 catalog and in the HD Extension Charts (Nesterov et al. 1995) whereas the latter were measured for 10 stars (see Sect. 2.2).

The Tycho-2 proper motions are based on the comparison

between contemporary mean positions derived from the recent Tycho observations on-board Hipparcos and early-epoch positions observed many decades ago (see Høg et al. 2000 and references therein). Due to the long time-baseline they have rather high precision and therefore directly indicate the long-term mean tangential motions of the stars. We have collected proper motion components for 53 stars in a field 20' around the center of NGC 1582. They are shown in the vector point diagram in Fig. 4a. The points distribution is characterized by a

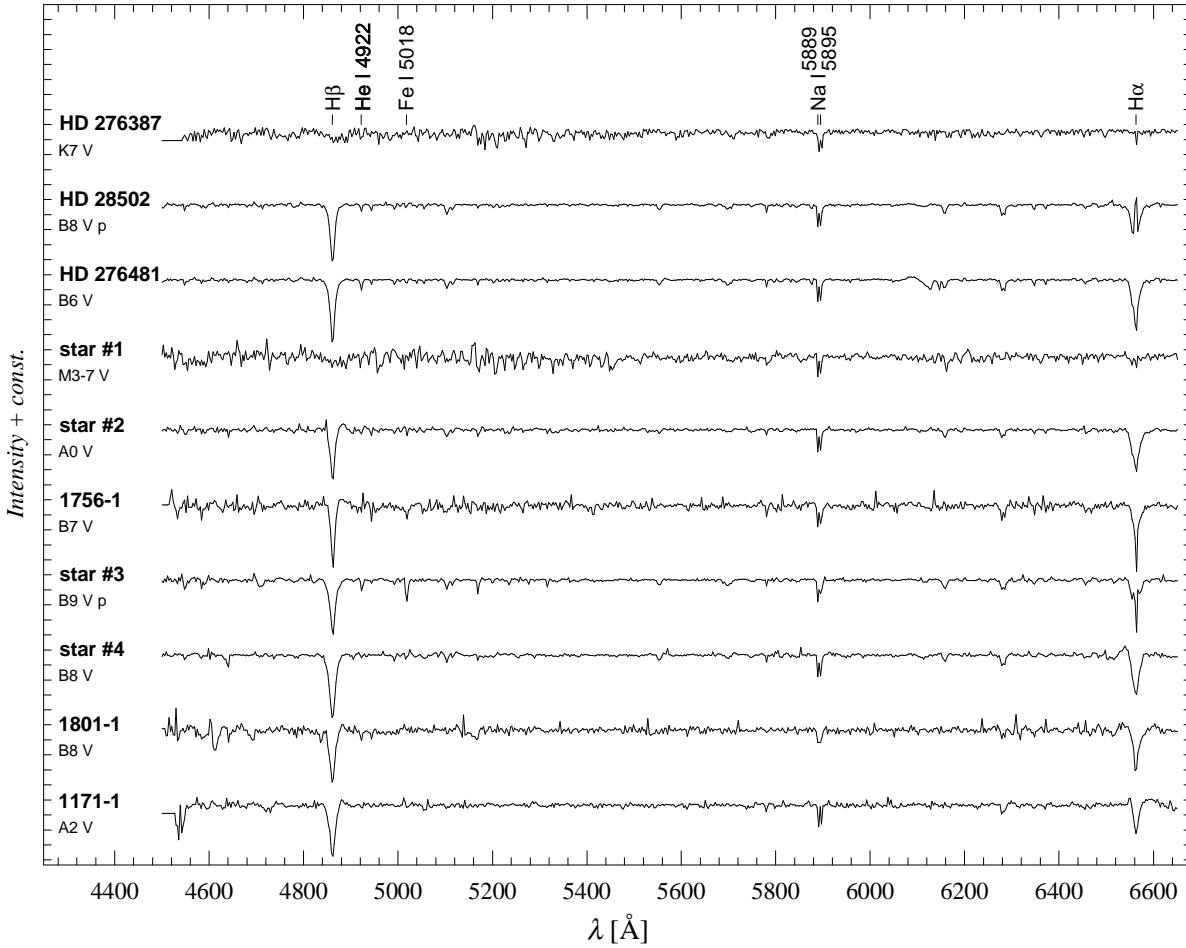


Fig. 5. Spectra of a sample of bright stars in the field of NGC 1582. A few interesting lines are indicated. See Table 3 for details.

global spread ~ 10 mas/yr with a noticeable concentration, which seems to indicate a possible physical relation among these stars.

Spectra obtained with the Echelle spectrograph allow us to get radial velocity, as described in Sect. 2.2. The obtained values are shown in Fig. 4b, and range from -40 to +40 km/s.

3.3. Photometric diagrams

The color-color diagrams (CCDs) and the color-magnitude diagrams (CMDs) are shown in Figs. 6, 7 and 8. The first two figures include all the stars measured in the direction of NGC 1582 and also several bright stars with available spectral classification and Hipparcos (ESA 1997) or Tycho-2 magnitudes within $20'$ from the cluster center and not covered by our photometry. Tycho-2 magnitudes are converted to the Johnson system using the relations given by Bessell (2000) and approximated ($U - B$) and ($V - I$) colors are obtained according to the spectral types (when they are available) together with Schmidt-Kaler (1982) and Cousins (1978a,b) calibrations. Fig. 8 presents the CMDs from 2MASS catalog for

stars placed inside the cluster radius ($R < 15'$, see Sect. 3.1) and for star placed in a ring around the cluster ($20' < R < 25'$, see Fig. 3) that is adopted as a comparison field. Radii are selected in such a way that both diagrams in Fig. 8 cover equal sky areas.

If we inspect Fig. 6a and compare the star positions with Schmidt-Kaler's (1982) Zero Age Main Sequence (ZAMS), using different reddening values, there seem to be two populations: one having a lower excess (dashed curve) mainly defined by the brightest stars, and another one with a much larger reddening. We claim that the former define the open cluster NGC 1582, whereas the latter population is identified as the Galactic disk component, made of stars placed at different distances and with a different amounts of absorption. To guide the eye we have placed another ZAMS reddened by $E_{B-V} = 1.2$ (dotted curve). A similar conclusion can be deduced from Figs. 7 and 8, where we see that most of the stars observed are just Galactic disk field stars and NGC 1582 looks like a small group of stars brighter than $V \approx 14$ above the mean stellar background.

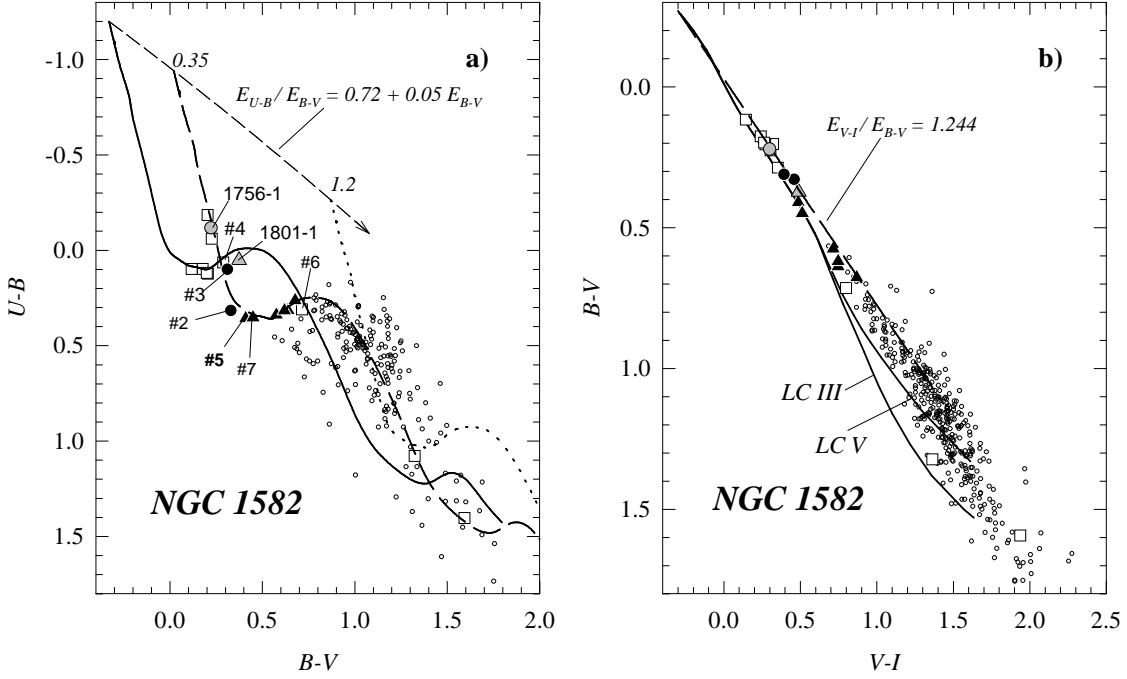


Fig. 6. Color-color diagrams (CCDs) of stars in the region of NGC 1582. **a)** $U - B$ vs. $B - V$ diagram. The symbols have the following meaning: big circles are adopted member stars (m), triangles are probable member stars (pm), empty squares are non-member stars (nm), and small open circles are stars without any membership assignment. Black symbols indicate stars with CCD measurements whereas grey ones are for stars with data from the Tycho-2 catalog. The solid line is Schmidt-Kaler's (1982) ZAMS, whereas the dashed and dotted lines are the same ZAMS, but shifted by $E_{B-V} = 0.35$ and 1.2 , respectively. The dashed arrow indicates the normal reddening path. **b)** $B - V$ vs. $V - I$ diagram. Symbols as in Fig. 5a. The solid lines represent the intrinsic positions for stars of luminosity classes V and III (Cousins 1978a,b). The dashed line gives the normal reddening path ($R = 3.1$).

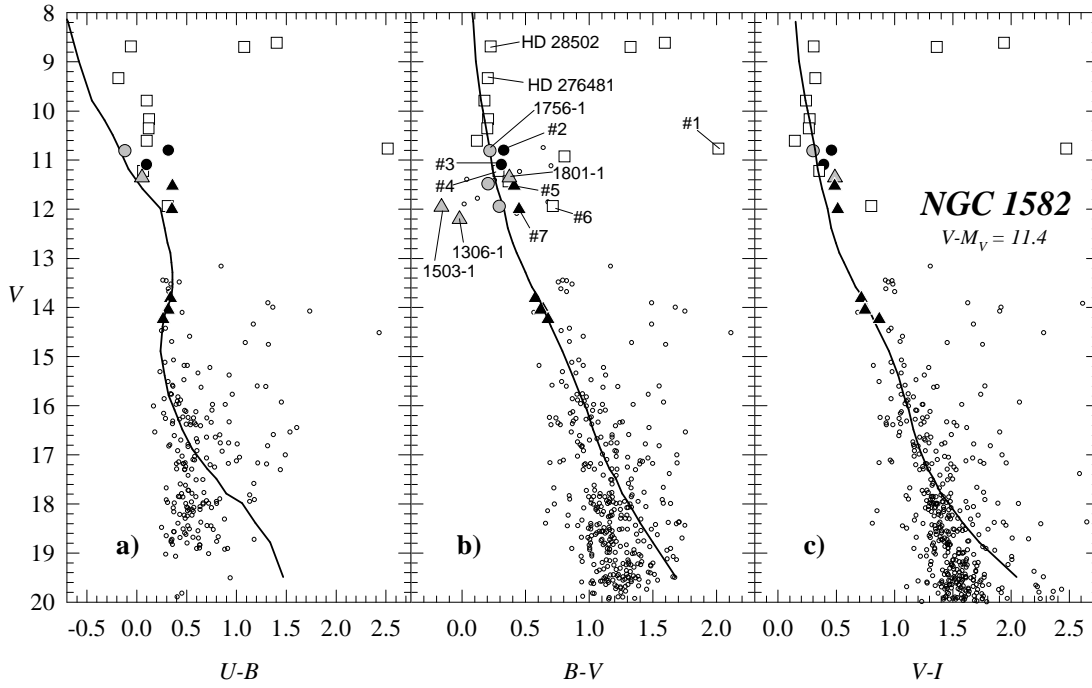


Fig. 7. CMDs for all the stars covered in the field of NGC 1582. Symbols as in Fig. 5a. The solid line is the Schmidt-Kaler (1982) empirical MS fitted to the apparent distance modulus $V - M_V = 11.4$ ($V - M_V = V_0 - M_V + 3.1E_{B-V}$, see Sect. 3.4).

3.4. Members selection

We derive cluster membership by comparing the distribution of the stars in the different photometric diagrams (e.g. Baume et al. 1999, Ortolani et al. 2002, Carraro 2002b). But we also take into account their location in the finding chart (Fig. 2), in the vector point diagram and the measured radial velocities (Fig. 4). At first, we use only Figs. 6 and 7 and we notice that there are five bright blue stars (#2, 3, 4, 5 and 7) that fit pretty well the empirical ZAMS shifted by $E_{B-V} = 0.35$ (dashed line). These stars also are well placed in the vector point diagram, although three of them, stars #4, 5 and 7, slightly depart from the central concentration in this diagram. Additionally, star #4 has a radial velocity value very different from that of stars #2 and 3. Therefore, stars #2 and 3 are adopted as cluster members (*m*), stars #5 and 7 as probable members (*pm*), and star #4 is considered to not belong to the cluster (*nm*).

Using stars #2, 3, 5 and 7, we compute colour excess values for each of them applying the relations $E_{U-B}/E_{B-V} = 0.72 + 0.05 E_{B-V}$ and $(U - B)_0 = 3.69 (B - V)_0$ according to Vázquez & Feinstein (1991), this yields a mean value $E_{B-V} = 0.35 \pm 0.03$ (*s.d.*), here adopted as the cluster color excess. Beside, following the reddened ZAMS path onto CCDs and CMDs, we select four additional stars and adopt them as probable cluster members (*pm*).

Star #2 is of spectral type A0 V, as derived from its spectrum and from its position in the CCD. However by comparing its position in the CMDs with respect to other members, we notice that it appears over-luminous by 0.75 mag. This can be explained by assuming it is a binary system. Of course, this is only a suggestion, which can be confirmed for instance by looking for radial velocity variations in other-epoch spectra. Therefore we keep it on the adopted members list. On the other hand, star #6 is well placed on the CCDs (see Fig 6) as a F-type star, but its position in the CMDs (see Fig. 7) contradicts this hypothesis and it is therefore considered a non-member (*nm*).

At this point, we are ready to use Fig. 8 as well. In this figure we superimpose to the data an empirical Main Sequence (MS) obtained by the combination of the Schmidt-Kaler (1982) and Koornneef (1983) calibrations shifted according to the relation among colors obtained from the van de Hulst extinction curve #15 (Johnson 1968). By closely inspecting this figure, we notice that there are some stars not covered by our survey, but within the cluster radius, which are properly located both in the CMD (Fig. 8a) and in the proper motion diagram of Fig. 4a (grey symbols in those figures), and one of them (TYC 2892-1756-1) also has a radial velocity value compatible with those of adopted member stars #2 and 3 (see Fig. 4b). This group of stars has a counterpart in the corresponding comparison field (Fig. 8b). We compute then the *J* distributions for stars with $J - K < 0.2$ (see Table 4) in each diagram and we compare them by

using a χ^2 test. We find that they are different with a probability higher than 95 %. Therefore, although we are aware that we are dealing with small numbers of stars and that a statistical analysis is therefore only indicative, the difference between both distributions turns out to be noticeable and therefore we are inclined to consider the group of stars mentioned above as cluster members (*m*). An exception are stars TYC 2892-1306-1, TYC 2892-1503-1 and TYC 2892-1801-1. The first two have high errors in their $B - V$ measurements and are situated leftward of the MS in Fig. 7b, and the third has a radial velocity value with a huge error and is far from the adopted values for cluster members (see Fig. 4b and Table 3). We cannot exclude that this might be due to a binary effect. Thus we consider these three particular stars as only probable members (*pm*). On the other hand, the photometric diagrams also reveal that some stars with available spectral classification and Tycho-2 data do belong to the field stellar population; they are therefore taken as non-members (*nm*).

Star #1 (GSC 02892-01209) deserves special attention. It is the brightest and one of the reddest stars in our sample. Unfortunately, we were not able to find out either its distance or its proper motion components. This star might in principle be a giant cluster member. However, from its spectrum we obtained a radial velocity value that disagrees with the adopted one for adopted cluster members (see Fig 4b). Also, it is classified as a M-type star and its parameters (reddening and distance) differ from those of the cluster ones ruling out the possibility that it is a member star.

In conclusion, after the above detailed analysis of the brightest stars in the NGC 1582 region, we conclude that *i*) the brightest ones are merely field stars, and *ii*) we only consider the stars classified as *m* and *pm* as the main members of the open cluster NGC 1582. They are indicated in Fig. 2, and demonstrate that we are dealing with a sparse, poor and severely field-star-contaminated open cluster.

3.5. Hints for distance and age

In Fig. 9 we plot the reddening-corrected M_V vs. $(B - V)_0$ diagram for the cluster members and probable cluster members adopting a distance modulus of $V_0 - M_V = 10.3 \pm 0.2$ (error from inspection). Last value fits very nicely the empirical Schmidt-Kaler (1982) ZAMS. We also apply the spectroscopic parallax method to three classified stars, obtaining $V_0 - M_V = 9.9 \pm 0.2$. These values are in quite good agreement and imply that the few stars identified as NGC 1582 are located 1100 ± 100 pc away from the Sun in the outer edge of the Orion arm.

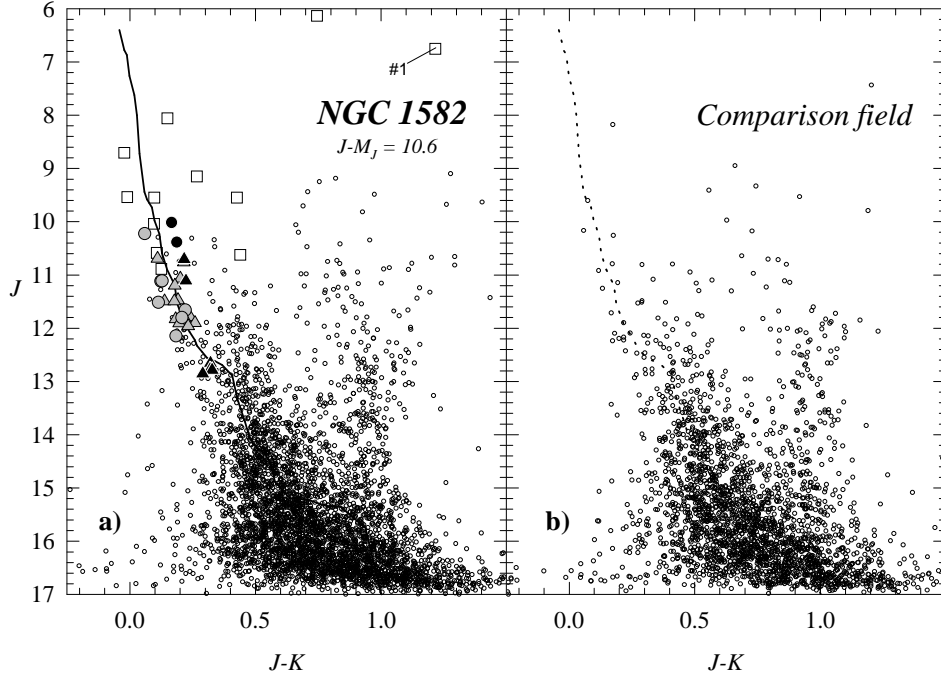


Fig. 8. CMDs from 2MASS catalog. Symbols are as in Fig. 6a. **a)** Stars placed inside the cluster area. **b)** Stars placed in a ring around the cluster. The solid line in panel **a)** and the dotted one in panel **b)** are the intrinsic position for MS stars from the Schmidt-Kaler (1982) and Koornneef (1983) calibrations fitted to the apparent distance modulus $J - M_J = 10.6$ ($J - M_J = V_0 - M_V + (3.1 - 2.3)E_{B-V}$, see Sect. 3.4).

Table 4. J magnitude distributions from stars with $J - K < 0.2$ in Fig. 8.

ΔJ	8-9	9-10	10-11	11-12	12-13
<i>Cluster</i>	2	3	16	20	22
<i>Comparison field</i>	1	1	4	7	6

From the obtained spectral classification (see Table 3) and from the location of adopted cluster members stars in Fig. 5a along the shifted ZAMS (dashed curve), we infer that the spectral types range from B7 to F2. If the stars having B7 spectral type are still on the main sequence, we derive an age of about 300 Myr for NGC 1582 (Girardi et al. 2000). A similar result is obtained by the isochrone fitting method shown in Fig. 9.

4. NGC 1663

NGC 1663 (= OCL 461 = C0445+130) is located quite high above the galactic plane for an open cluster (see Table 1) and does not emerge much from the general Galactic field toward its direction. According to Lyngå (1987) it has a diameter of 12' and therefore our observations cover most of the cluster region (see Fig. 10). Unfortunately, proper motions are available only for four stars in the region 10' around NGC 1663 (see Table 5), so we must rely mostly on photometric data to derive

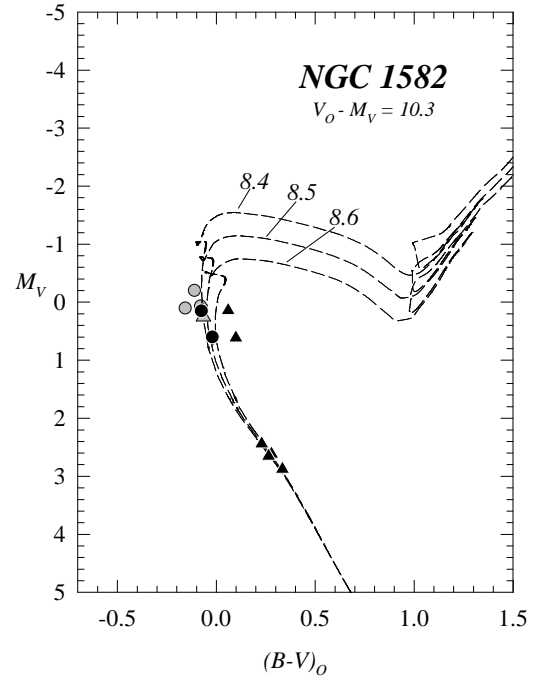


Fig. 9. M_V vs. $(B - V)_0$ diagram of the members and probable members in the region of NGC 1582. Symbols as in Fig. 6a. Dashed curves are the isochrones from Girardi et al. (2000). The reported numbers give the $\log(\text{age})$.

cluster members and cluster fundamental parameters.

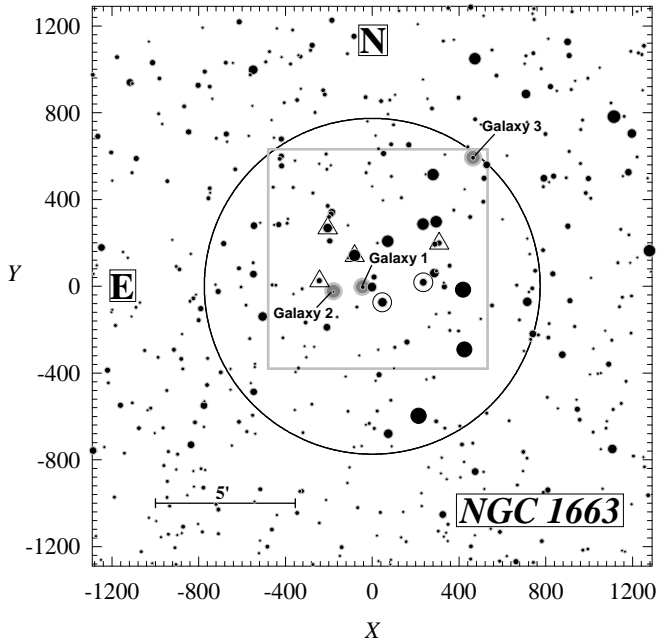


Fig. 10. Finding chart of the NGC 1663 region ($20' \times 20'$ and J filter). The black solid circle, $6'$ radius, indicates the adopted angular size for the cluster (see Sect. 4.1 and Fig. 10). As in Fig. 2, grey square indicates the area covered from Asiago, and adopted members and probable members are enclosed in small circles and triangles, respectively. For a coordinate reference, the center ($X = 0$; $Y = 0$) corresponds to the cluster coordinates (see Table 1), and each X - Y unit is $0''.465$. Field galaxies positions are indicated as grey circles.

4.1. Stellar counts

NGC 1663 appears as a loose aggregate of a few relatively bright stars. As for NGC 1582, we perform stellar counts in concentric rings around the cluster center, but this time, since the cluster does not appear much extended, we only use the DSS-2 red data. The stellar density profile is shown in Fig. 11. One can readily see the lack of any clear trend, and therefore it is a difficult task to define the cluster radius. Anyway, if we inspect the DSS-2 image, the region where is located the over-density of stars is about $6'$ radius (see Fig. 10). In conclusion, it is hard to decide upon the real nature of this cluster, although, broadly speaking, the over-density we found seems to suggest that we are looking at an aggregate of the kind suggested by Bica et al. (2001), namely a POCR. The lack of an unambiguous cluster center, and the loose distribution of the brightest stars across the field support this suggestion.

4.2. Photometric diagrams and member selection

We follow the same method applied above for NGC 1582 to derive preliminary individual reddening

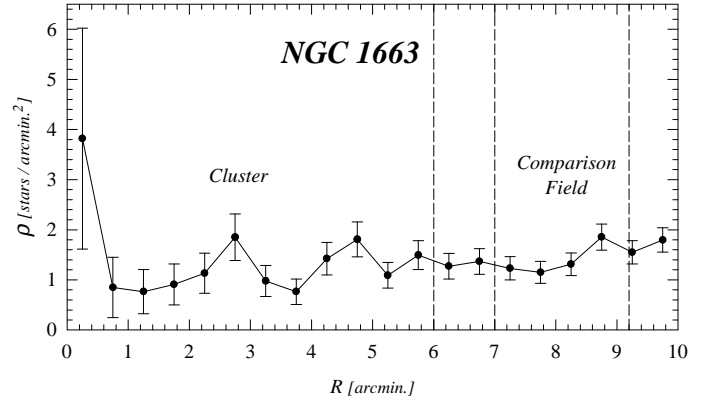


Fig. 11. Stellar densities in the region of NGC 1663 as a function of the radius from DSS-2 image. The dotted lines indicate the adopted limits for the cluster and for the comparison field related with Fig. 14b.

and membership of the cluster. Photometric diagrams are shown in Fig. 12, 13 and 14, where all the observed stars are presented in the first two, whereas the last one is obtained from 2MASS data. Let us fix our attention on Fig. 12a: here all the stars seem to crowd along an empirical ZAMS shifted by $E_{B-V} = 0.20$. It is however clear that in this case a reddening solution can not be found, since all the stars lie well beyond the location of A5 spectral type stars (Ortolani et al. 2002). The low color excess and the small dispersion in reddening are not unexpected, due to the position of the cluster high above the Galactic plane and toward the anti-center direction. The CMDs are not easy to interpret, since most of the stars are just Galactic disk field stars, as is readily seen by inspecting both panels in Fig. 14. From this figure it is evident that NGC 1663 emerges as an over-density of a dozen stars brighter than $V \approx 16 - 17$ above the mean stellar background.

In conclusion, only preliminary membership information can be derived from the CMDs of Figs. 13 and 14. We therefore try to fit the distribution of the stars with both the empirical Schmidt-Kaler (1982) ZAMS and with several isochrones from Girardi et al. (2000) by conservatively assuming that the metal content is solar. A possible relationship might exist between some MS stars and the brightest star (star #1). This is the star HD 287125 with spectral type G5 and it could be a giant cluster member, but its parallax value (see Table 5) definitely rules out this possibility, and we are left with a nearby foreground star. The shape of the upper part of the CMDs seems to suggest that the turn-off point (TO) is located at about $V = 13.2$, $B - V = 0.6$, and that the stars rightwards of the TO are sub-giant stars. On this basis we will consider two stars as cluster members (m), four more as probable ones (pm) and a few bright ones were identified as non-members (nm).

Fig. 13 shows the CMDs corresponding to the cluster area, and to a ring around it adopted as a comparison field (see Fig. 11). As in Fig 9 for NGC 1582, radii were

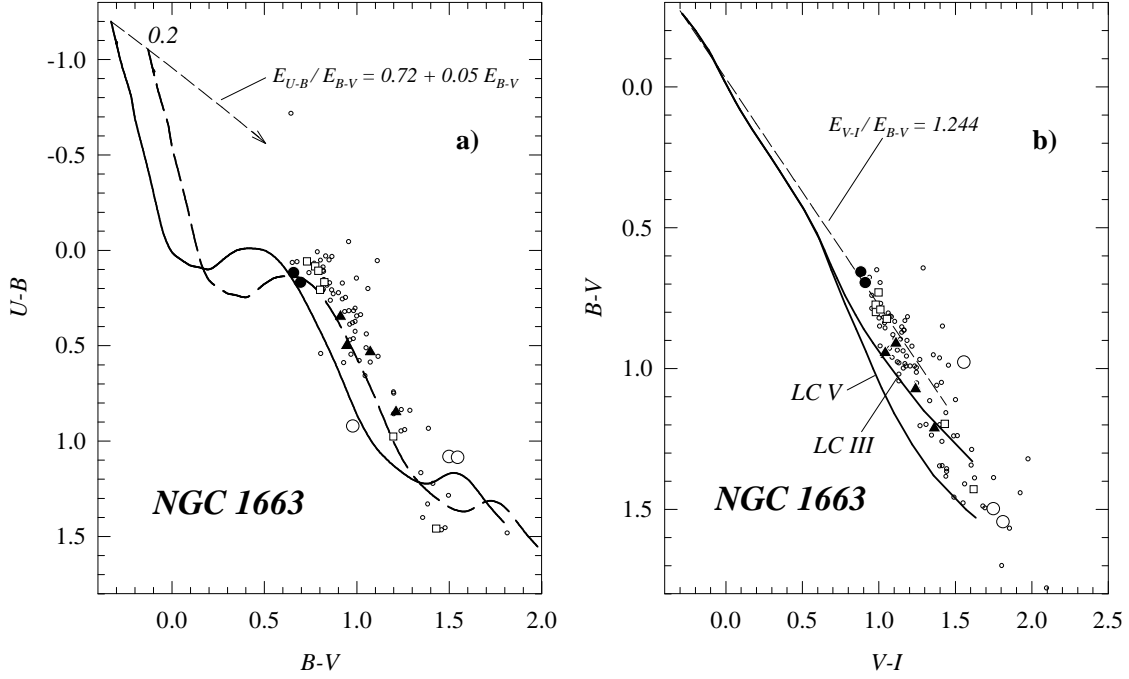


Fig. 12. CCDs of the stars in the region of NGC 1663. **a)** $U - B$ vs. $B - V$ diagram. As for NGC 1582, symbols have the following meaning: circles are adopted member stars (m), triangles are probable member stars (pm), empty squares are non-members stars (nm) and small open circles are stars without any membership assignment. Field galaxies are indicated as white circles. The solid line is Schmidt-Kaler's (1982) ZAMS, whereas the dashed one indicates the same ZAMS, but shifted by $E_{B-V} = 0.2$. The dashed arrow indicates the normal reddening path. **b)** $B - V$ vs. $V - I$ diagram. Symbols as in Fig. 12a. The solid lines are the intrinsic positions for stars of luminosity classes V and III (Cousins 1978a,b), while the dashed one provides the normal reddening path ($R = 3.1$).

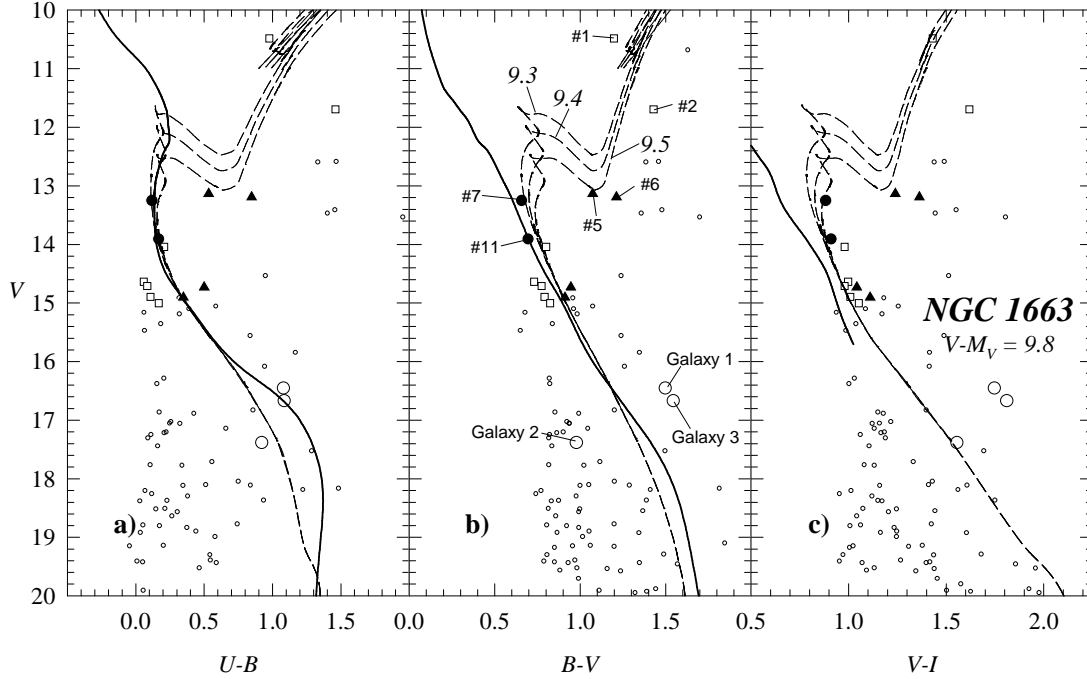


Fig. 13. Color-magnitude diagrams (CMDs) for all the stars covered in the field of NGC 1663. Symbols as in Fig. 12a. The solid line and dashed curves are the Schmidt-Kaler (1982) empirical ZAMS and isochrones from Girardi et al. (2002) respectively. They were fitted to the apparent distance modulus $V - M_V = 9.8$ ($V - M_V = V_0 - M_V + 3.1 E_{B-V}$, see Sect. 4.2). The numbers indicate $\log(\text{age})$.

Table 5. Some bright stars in the field of NGC 1663.

#	2MASS ID. Tycho-2 ID. HD/GSC ID.	X Y	α_{2000} δ_{2000}	V	$B - V$ $U - B$ $V - I$	J	$J - K$	$\mu_{\alpha} \cos(\delta)$ μ_{δ} $Parallax$	Memb.
1	J0449107+130612 TYC 691-633-1 HD 287125	426.5 -292.5	04:49:10.7 13:06:12.1	10.48	1.20 0.98 1.43	8.09	0.71	13.1 ± 1.5 -12.4 ± 1.5 108.4 ± 46.3	<i>nm</i>
–	J0448489+131432 TYC 695-519-1 –	1115.0 780.6	04:48:48.9 13:14:32.2	10.47 _T	0.49 _T – –	9.14	0.38	22.2 ± 1.4 -36.8 ± 1.4 –	–
–	J0449174+130349 TYC 691-133-1 –	213.6 -597.8	04:49:17.4 13:03:49.6	10.68 _T	1.63 _T – –	7.96	0.92	6.6 ± 2.3 -2.5 ± 2.3 –	–
2	J0449109+130819 TYC 695-27-1 GSC 00695-00027	419.0 -17.6	04:49:10.9 13:08:19.9	11.69	1.43 1.46 1.62	8.98	0.83	3.5 ± 3.1 -1.4 ± 3.1 –	<i>nm</i>
5	J0449308+131030 – –	-205.2 266.9	04:49:30.8 13:10:30.7	13.13	1.07 0.53 1.24	11.06	0.65	– – –	<i>pm</i>
6	J0449269+130932 – –	-81.3 140.3	04:49:26.9 13:09:32.1	13.19	1.21 0.85 1.36	10.88	0.69	– – –	<i>pm</i>
7	J0449227+130752 – –	47.4 -74.5	04:49:22.7 13:07:52.2	13.25	0.66 0.12 0.88	11.79	0.39	– – –	<i>m</i>
11	J0449167+130835 – –	235.7 17.1	04:49:16.7 13:08:35.4	13.91	0.70 0.17 0.91	12.44	0.40	– – –	<i>m</i>
16	J0449320+130837 – –	-242.9 24.1	04:49:32.0 13:08:37.6	14.73	0.94 0.50 1.04	13.01	0.46	– – –	<i>pm</i>
18	J0449144+130959 – –	308.6 197.7	04:49:14.4 13:09:59.5	14.91	0.91 0.35 1.11	13.07	0.52	– – –	<i>pm</i>

Notes:

- Letters *T* indicate data obtained from Tycho-2 catalog.
- Proper motion and parallax values are expressed in mas/yr and mas respectively.

selected in such a way that both diagrams in Fig. 14 represent equal sky areas. By comparing both diagrams we can see a notable over-density of bright stars in the cluster region, which would favor the idea that NGC 1663 is a physical cluster.

4.3. Hints for NGC 1663 distance and age

As discussed in the previous section, Fig. 13 allows us to derive a rough estimate of the distance and the age of NGC 1663. These diagrams yield a cluster distance of about 700 pc ($V_0 - M_V = 9.2 \pm 0.2$) and an age of about 2000 Myr ($\log(age) = 9.4$). We also tried other combinations of distance moduli and color excesses over the CMDs, in order to check whether the reddest stars could be cluster members, but the obtained solutions did not agree at all with the corresponding CCDs of Fig. 12. In conclusion, if NGC 1663 really is a star cluster, we may be facing a dissolving aggregate of the kind proposed

by Bica et al. (2001).

5. Field galaxies

Since NGC 1663 is located well above the Galactic plane, it is not very improbable that we should observe field galaxies toward its direction. In our case three of them are clearly detectable and we notice that they were not catalogued so far, except for entries in the 2MASS catalog as point sources. Therefore, we compute their integrated photometric parameters by performing aperture photometry. We use the PHOT task at increasing radius until the resulting magnitudes converged. Our results are presented in the photometric diagrams and in Table 6 together with an estimate of their angular sizes and a preliminary morphological classification that - by the way - agrees quite well with the observed colors.

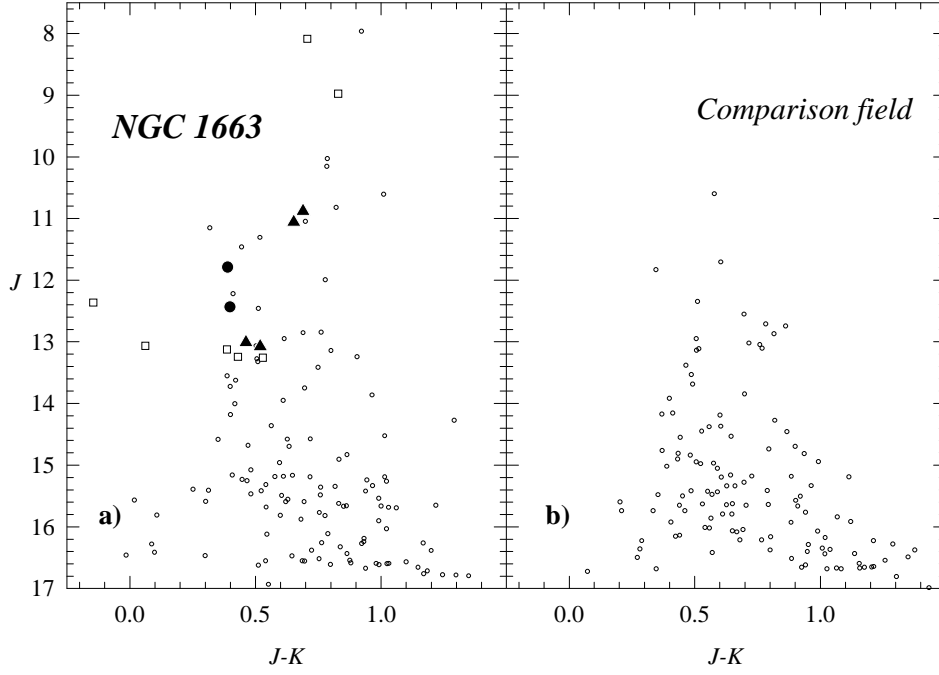


Fig. 14. CMDs from the 2MASS catalog. Symbols as in Fig. 12a. **a)** Stars placed inside the cluster area **b)** Stars placed in a ring around the cluster (see Fig. 10).

Table 6. Galaxies observed in the field of NGC 1663

Name 2MASS ID	α_{2000} δ_{2000}	Morphology $D \times d$	V	$B - V$ $U - B$ $V - I$	J H K
Galaxy 1	04:49:25.7	$E3$	16.45	1.50	14.52
J0449257+1308	13:08:25.0	$17.8'' \times 13.3''$		1.08	13.76
				1.75	13.49
Galaxy 2	04:49:29.9	$S0$	17.38	0.98	16.33
J0449299+1308	13:08:15.4	$23.1'' \times 9.4''$		0.92	15.85
				1.56	14.57
Galaxy 3	04:49:09.5	$E0$	16.67	1.55	14.82
J0449095+1313	13:13:03.0	$13.5'' \times 13.5''$		1.09	13.99
				1.81	13.54

6. Conclusions

We have presented the first CCD multicolor study in the regions of the two poorly known northern open clusters NGC 1582 and NGC 1663 for which no investigations had been carried out insofar. In the case of NGC 1582 we also obtained Echelle spectra of the brightest stars. In detail, we found that:

- NGC 1582 is a very poor and spread-out cluster with a radius of $15'$ and formed by a group of stars at a distance of about 1 kpc in the outer edge of the Orion arm. We estimate that its reddening is $E_{B-V} = 0.35 \pm 0.03$ and that it has an age of about 300 Myr. We also obtained radial velocities for 10 stars and detected two probable binary systems among its members.
- NGC 1663 has a lower reddening of $E_{B-V} = 0.2$ but, until more robust definition of its membership is avail-

able, the interpretation of the CMDs is quite difficult. We only derive a preliminary membership assignment and we suggest this object has an age of ~ 2000 Myr and a distance value of about 700 pc. The most probable interpretation of the data at our disposal is that NGC 1663 is an open cluster remnant.

Finally, we identify three previously unclassified field galaxies in the direction of NGC 1663. We provide their integrated magnitudes and colors, angular sizes and preliminary morphological types. Two of them are found to be ellipticals and the third is either a flattened S0 or a spiral one.

This article is partially based on the Second Generation Digitized Sky Survey that was produced at the Space Telescope Science Institute under US government grant

NAG W-2166. The images of these surveys are based on photographic data obtained using the Oschin Telescope on Palomar Mountain and the UK Schmidt Telescope. The plates were processed into the present compressed digital form with the permission of these institutions. This study has also made use of: a) the SIMBAD database, operated at CDS, Strasbourg, France, and b) the data from the Two Micron All Sky Survey, which is a joint project of the University of Massachusetts and the Infrared Processing and Analysis Center, funded by NASA and NSF

Acknowledgements. The authors acknowledge the Asiago Observatory staff for the technical assistance. Fruitful discussion with Roberto Barbon, Ruggero Stagni, Corrado Boeche and Silvano Desidera are also warmly acknowledged. We thank the anonymous referee for the detailed report which helped to significantly improve the paper presentation. The work of GB is supported by Padova University through a postdoctoral grant.

References

- Baume G., Vázquez R.A. & Feinstein A. 1999, A&AS 137, 233
 Bessel M.S. 2000, PASP 112, 961
 Bica E., Santiago B.X., Dutra C.M., et al. 2001, A&A 366, 827
 Carraro G. 2002a, A&A 387, 479
 Carraro G. 2002b, MNRAS 331, 785
 Cousins A.W.J. 1978a, MNSSA 37, 62
 Cousins A.W.J. 1978b, MNSSA 37, 77
 Desidera S., Fantinel D., & Giro E. 2002, AFOSC USER MANUAL
 Dias W.S., Alessi B.S., Moitinho A., et al 2002, A&A 389, 871
 ESA 1997, The Hipparcos and Tycho Catalogs, ESA SP-1200
 Girardi L., Bressan A., Bertelli G., & Chiosi, C. 2000, A&AS 141, 371
 Johnson H.L. 1968, In Nebulae and Interstellar matter. Middlehurst B.M & Aller L. (eds.). Univ. of Chicago Press, p. 167
 Høg E., Fabricius C., Makarov V.V. et al. 2000, A&A 357, 367
 Jaschek C., Jaschek M., 1987, *The classification of stars*, Cambridge University Press
 Koornneef J. 1983, A&A 128, 84
 Landolt A.U. 1992, AJ 104, 340
 Lyngå G. 1987, Catalog of Open Star Cluster Data, Strasbourg, CDS
 Montes D., Martin E.L., Fernandez-Figueroa M.J., et al. 1997, A&AS 123, 473
 Montes D., Ramsey L.W., & Welty A.D., 1999, ApJS 123, 283
 Munari U. & Zwitter T., 1994, Padova and Asiago Obs. Tech. Rep. 4
 Nesterov V.V., Kuzmin A.V., Ashimbaeva N.T. Volchkov A.A. Roeser S & Bastian U. 1995, A&AS 110, 367
 Ortolani S., Carraro G., Covino S., et al. 2002, A&A 391, 179
 Patat F., Carraro G. 2001, MNRAS 325, 1591
 Schmidt-Kaler Th. 1982, Landolt-Börnstein, Numerical data and Functional Relationships in Science and Technology, New Series, Group VI, Vol. 2(b), K. Schaifers and H.H. Voigt Eds., Springer Verlag, Berlin, p.14
 Stetson P.B. 1987, PASP 99, 191
 Vázquez R.A. & Feinstein A. 1991, A&AS 90, 317